A large-scale multi-centre cerebral diffusion tensor imaging study in amyotrophic lateral sclerosis

[1]H-P Müller, [2]MR Turner, [3]J Grosskreutz, [4]S Abrahams, [5]P Bede, [6]V Govind, [7]J Prudlo, [1]A C Ludolph, [8]M Filippi, [1]J Kassubek
for The Neuroimaging Society in ALS (NiSALS) DTI Study Group

[1]Department. of Neurology, University of Ulm, Ulm, Germany
[2]University of Oxford Nuffield Department of Clinical Neurosciences, John Radcliffe Hospital, Oxford, United Kingdom
[3]Hans-Berger Department of Neurology, Jena University Hospital, Jena, Germany
[4]Human Cognitive Neuroscience, Psychology–PPLS & Euan MacDonald Centre for MND Research & Centre for Cognitive Aging and Epidemiology, University of Edinburgh, Edinburgh, United Kingdom
[5]Quantitative neuroimaging group, Academic Unit of Neurology, Trinity College Dublin, Dublin, Ireland.
[6]Department of Radiology, University of Miami School of Medicine, Miami, Florida, United States of America
[7]Department of Neurology, University of Rostock and DZNE, Rostock, Germany
[8]Neuroimaging Research Unit, Institute of Experimental Neurology, Division of Neuroscience, San Raffaele Scientific Institute, Vita-Salute San Raffaele University, Milan, Italy

Corresponding author: Prof. Dr. Jan Kassubek
Department of Neurology, University of Ulm
Oberer Eselsberg 45, 89081 Ulm, Germany
phone + 49 731 1771206
email jan.kassubek@uni-ulm.de

Running title: Multi-centre DTI in ALS

Key words: Biomarker, diffusion tensor imaging, motor neuron disease, neurodegenerative disease, neuroimaging

Abstract

Diffusion tensor imaging (DTI) has enabled to visualize the cerebral tissue structural connectivity of the neurodegenerative disorder amyotrophic lateral sclerosis (ALS), which extends beyond the motor pathways. The effective translation of DTI metrics as biomarkers requires its application across multiple magnetic resonance imaging (MRI) scanners and patient cohorts. A multi-centre study was undertaken to address the challenges of DTI data analysis and to assess structural connectivity in ALS at a large sample size.

Four hundred and forty two DTI data sets from patients with ALS (N=253) and control subjects (N=189) were collected from eight ALS-specialist clinic sites (Dublin, Ireland; Edinburgh, UK; Jena, Germany; Miami, US; Milano, Italy; Oxford, UK; Rostock, Germany; Ulm, Germany). The magnetic field strength, MRI scanner manufacturer and DTI protocols varied across the sites. Fractional anisotropy (FA) maps of the control subjects were used to establish correction matrices to pool data between the sites, and correction algorithms were applied to the FA maps of the control and ALS patient groups.

Single-site analysis showed a characteristic pattern of FA reduction in the corticospinal tracts at the group level. After pooling of data sets from all centres, whole-brain-based statistical analysis of FA maps not only confirmed the most significant alterations in the corticospinal tracts, but also captured additional significant white matter tract changes in the frontal lobe, brainstem and hippocampal regions of the ALS group, in keeping with *post mortem* neuropathological stages. A stratification of the ALS group for disease severity (ALS functional rating scale) confirmed these findings.

Overcoming the challenges associated with multi-platform, multi-centre data processing and analysis, this large-scale study effectively demonstrated the DTI-based fingerprint of ALS that includes extensive extra-motor involvement. This success paves the way for the use of DTI-based metrics as potential read-outs in natural history, prognostic stratification and multi-site disease-modifying studies in ALS.

Introduction

The use of advanced magnetic resonance imaging (MRI) techniques, in particular diffusion tensor imaging (DTI) of white matter tracts, has greatly improved the understanding of the *in vivo* cerebral and spinal neuropathology of the adult neurodegenerative disorder amyotrophic lateral sclerosis (ALS) (Agosta *et al.*, 2010; Bede and Hardiman, 2014; Kassubek *et al.*, 2012; Keil *et al.*, 2012; Turner *et al.*, 2012). DTI can quantify the integrity of large white matter tracts *in vivo* using metrics such as fractional anisotropy (FA) (Le Bihan *et al.*, 2001). A DTI-based *in vivo* imaging concept has also been applied to the recently introduced neuropathological staging system, indicating that ALS may disseminate in regional patterns (Brettschneider *et al.*, 2013; Kassubek *et al.*, 2014). ALS overlaps with frontotemporal dementia both clinically and pathologically. While the majority of ALS patients do not develop a frank dementia, a large proportion show cognitive impairments on the same spectrum, and DTI has demonstrated extension of white matter changes into frontal and temporal lobes accordingly (Pettit *et al.*, 2013; Sarro *et al.*, 2011).

Imaging biomarkers are urgently required for future pharmaceutical trials to be used as objective study end-points. The development of robust prognostic and diagnostic markers has become a major research priority in this notoriously heterogeneous disorder (Turner *et al.*, 2009; Turner *et al.*, 2015). With this has come the realisation that effective biomarkers, particularly those integrated in therapeutic studies, will need to be applicable across multiple international centres that, in the case of MRI, may vary in their scanner hardware and sequence acquisition parameters.

Following the success of the Alzheimer's Disease Neuroimaging Initiative (ADNI), the Neuroimaging Society in ALS (www.nisals.org) was established in 2010 and developed a roadmap for the eventual standardisation and harmonisation of advanced MRI data in ALS (Turner *et al.*, 2011). The most sensitive cerebral pathology found in cross-sectional MRI studies in ALS patients has been in the white matter tracts (Menke *et al.*, 2014), in contrast to the characteristic hippocampal atrophy that largely defines Alzheimer's Disease. To date, there have been very few large-scale multi-site studies of DTI data, and none in ALS. Such studies may be hampered by differences in scanning protocols (Vollmar *et al.*, 2010; Teipel *et al.*, 2011), so an approach to pool DTI data acquired with different protocols was sought. The objective was to define alterations in the white matter structural connectome in ALS in a large scale patient cohort from multiple sites spread across the world.

To this end, a strategy is presented that should pave the way to use the large numbers of DTI data sets from local data bases of different study sites for comprehensive large-scale multicentre imaging studies.

Methods

Subject populations and scanning protocols

Four hundred and forty two DTI data sets from patients with ALS (N=253) and control subjects (N=189) from eight ALS-specialist clinic sites (tertiary referral centres) were selected ex post facto (Dublin, Ireland; Edinburgh, UK; Jena, Germany; Miami, US; Milano, Italy; Oxford, UK; Rostock, Germany; Ulm, Germany). Site details, including number of subjects and DTI scanning protocols, are given in Table 1. All patients were diagnosed with ALS according to standard clinical criteria by experienced ALS neurologists. No patient had frank dementia. Severity of disease-related physical symptoms was measured by use of the revised ALS functional rating scale (ALS-FRS-R) (Cedarbaum et al., 1999) and ranged from 14 to 48 with a mean of 37 [illegible] (ascertainment).

Preprocessing and whole-brain-based voxelwise comparison

Data from each site underwent an assessment on completeness and, according to a standard analysis quality control (Müller and Kassubek, 2013b), corrupted gradient directions in single DTI data sets were excluded from further analysis (Müller at al., 2011). That way, specific image artifacts, e.g. susceptibility-induced geometric warping, physiological and bulk patient motion, and chemical shift artifacts could be removed from the single data sets. The application of this quality control and repair algorithm allowed that DTI data sets that contained some corrupted gradient directions did not have to be excluded from the study. Out of the 442 data sets in total, 27 had to undergo the quality repair function.

Following a standardized iterative stereotaxic normalization process, using study specific DTI template sets (Müller and Kassubek, 2013b), FA maps of all participating subjects were derived centrewise in Montreal Neurological Institute (MNI) stereotaxic standard space.

Cross-sectional group comparison analysis followed the procedure described in detail previously (Müller and Kassubek 2013b). Maps of FA were calculated from MNI-normalized DTI data, and a Gaussian smoothing filter of 8 mm FWHM was applied to the normalized individual FA maps. Then, voxelwise statistical comparison (whole-brain-based spatial statistics, WBSS) was performed between the ALS patient group and the corresponding control group by Student's t-test with correction for multiple comparisons using the false-discovery-rate (FDR) algorithm (Genovese et al., 2002) at $p < 0.05$ and a clustering procedure at a threshold cluster size of 512 voxels to reduce type I and type II errors (Müller et al., 2013a). Voxels with FA values below 0.2 were not considered for statistical analyses since cortical grey matter shows FA values up to 0.2 (Kunimatsu et al., 2004). Centerwise cross-sectional results are provided in Supplementary Figure 1. Single-site cross-sectional comparisons have already been reported in various studies (Foerster et al., 2013a, 2013b).

For the comparison of sites, a study-specific template set (b0 and FA) was created with equal

weighting of sites, ALS-patients, and controls; then stereotaxic normalization was performed repeatedly with these equally weighted templates.

Influencing factors of FA maps

Different factors may contribute to the variability of DTI data of control subjects and ALS patients. Although the precise influence of each source of variation could not be delineated, investigating group FA differences between patients and controls on systematic between-centre differences was used to decide whether pooling across centres was feasible (Müller et al., 2013a). Potential sources of variability directly or indirectly influence DTI metrics. Data from the eight centres differed especially in mean age of the subjects and in recorded voxel size. These two parameters directly influence FA, which is known to be decreased in elderly subjects (Salat et al., 2005; Lim et al., 2013) and, especially in complex fibre-tracking structures with different axonal directionalities, FA is decreased with larger voxel size (Oouchi et al., 2007). Further parameters like field strength (B0), echo time (TE), and number of gradient directions (GD) influence the signal-to-noise-ratio and thus indirectly influence FA-values. Furthermore, site-specific sources of variability on DTI metrics, e.g. scanner specific variability, environmental noise, specific factors such as scanning time might be present in single site studies but will only slightly influence comparisons at the group level (Müller et al., 2013a). Therefore, a strategy to regress out confounders in a two-step procedure was applied to controls' data.

First, the covariates age, voxel size, TE, number of GD, and B0 were regressed out in controls' FA maps, and a corrected FA-map set consisting of all controls' FA maps was derived (Figure 1). In a second step, comparison of controls' FA maps was performed sitewise and, if the number of significant voxels in the group comparison of controls was below a threshold of 10,000 voxels, centres were merged into centre-clusters. Finally, residual site-specific influences (timing of scan, phenotype variations within the diagnosis of ALS, site-specific environmental noise, etc.) were defined together as inter-site effects. In a final step, 3-D linear correction matrices were calculated and applied to the data sets from each centre (Rosskopf et al., 2015) (Figure 1).

Sitewise pooling of ALS patients' FA maps

For ALS patients' FA maps, the covariates voxel size, age, number of GD, B0, and TE were regressed out with the 3D covariate regression matrices that were derived from the controls' FA maps and site clusters were set up according to the classification derived for controls' FA maps. Afterwards, 3D linear correction matrices for site clusters were applied (Figure 1).

Results

Single-site voxelwise comparison of FA maps (WBSS)

The whole-brain-based voxelwise analysis of single centres' FA maps without correction of confounding multicentric factors showed FA decreases mainly localized along the CST (Supplementary Figure 1). From these single-site analyses, no alterations beyond the CST were detected.

Voxelwise correction of confounding factors

FA maps of controls showed significant correlations ($p < 0.05$, corrected for multiple comparisons) to the covariates voxel size, age, number of GD, B0, and TE (Supplementary Figure 2A, upper panel). After regressing out these covariates, only small clusters of significance remained. The application of the correction matrices to FA maps of ALS patients also reduced the dependency on the covariates voxel size, age, number of GD, B0, and TE (Supplementary Figure 2A, upper panel). Centres were merged into centre-clusters. That way centres 3b and 6 form a centre-cluster, and centres 3a, 5, and 7 form the reference centre cluster (Supplementary Figure 2B). Residual accompanying site-specific influences in between center clusters were corrected by 3D linear correction matrices using centre-cluster C as a reference (Supplementary Figure 2C).

The whole-brain-based analysis was performed both for uncorrected and for corrected FA maps of 253 ALS patients and 189 controls and demonstrated difference maps as displayed in Figure 2. Resulting alteration patterns were apparently very similar, but after correction a more symmetric pattern between hemispheres was revealed; furthermore, no FA increase clusters remained and the resulting cluster showed an increased interconnectivity.

Multi-site voxelwise comparison of FA maps (WBSS)

The whole-brain-based analysis was performed for corrected FA maps of 253 ALS patients and 189 controls demonstrated difference maps as displayed in Figure 3. Differences were connected within one large cluster covering an area of about 150,000 mm3 in the white matter $p < 0.05$, corrected for multiple comparisons. With respect to the tract specific analysis (Kassubek et al., 2014), major significances were found along the corticospinal tracts (CST, corresponding to neuropathological stage 1 (Brettschneider et al., 2013)), including the “horseshoe” configuration (in coronal slicing) reflecting superior CST and transcallosal interconnecting fibres (Filippini et al., 2010), frontal involvement including areas crossed by the corticopontine and corticorubral tracts (neuropathological stage 2), and the corticostriatal pathway (pathological stage 3), pathways to brainstem (pontine/rubral involvement, pathological stage 2), and hippocampal areas including the proximal portion of the perforant path (pathological stage 4) (Figure 3A).

With the application of more lenient thresholding, a pattern resembling the neuropathological spreading could be demonstrated, beginning with highest significances (corrected $p < 0.0005$) in the upper CST, followed by clusters along the CST (corrected $p < 0.0001$), then including frontal areas (corrected $p < 0.001$), and at lowest significances (corrected $p < 0.005$) also including brain stem as well as hippocampal areas (Figure 3B).

Stratification of ALS patients was undertaken according to disability at the time of scan. Three age- and gender-matched groups which were homogeneously distributed over sites were selected: 38 patients with ALS-FRS-R ranging from 44 to 48 (m/f 20/18, mean age 62 years), 38 patients with ALS-FRS-R ranging from 31 to 43 (m/f 20/18, mean age 58 years), and 38 patients with ALS-FRS-R ranging from 14 to 30 (Figure 4). The group with mild ALS-FRS-R decrease showed a summed-up cluster of 11366 mm3 to be affected as significant FA decrease, the group with moderate ALS-FRS-R decrease showed in sum 26575 mm3 to be affected, and the group with moderate ALS-FRS-R decrease showed in sum 61707 mm3 of regional FA decreases.

After complete corrections for covariates and center differences, significant voxelwise correlation of FA values and ALS-FRS-R were observed along the CST ($p < 0.05$, corrected for multiple comparisons, Supplementary Figure 2). NB: correlation analysis for uncorrected FA maps did not show any significant clusters.

Discussion

This study has demonstrated that it is possible to meaningfully interpret combined DTI data from different MRI manufacturers and software platforms after application of appropriate compensations for site-specific differences. This might pave the way to repurpose larger numbers of DTI data sets of ALS patients for more clinically comprehensive large-scale multicentric imaging studies.

The results of this pooled analysis demonstrated extensive motor and extramotor white matter tract pathology in a large number of ALS patients compared to healthy controls. This is an important step in the development of DTI-derived biomarkers of neuropathology which are applicable across multiple sites.

Previous imaging studies have investigated ALS-related alterations of white matter with group sizes of typically 15-30 patients and healthy controls (Turner et al., 2012; Bede and Hardiman, 2014). These studies have consistently detected reduced FA (and concurrently increased radial diffusivity) within the rostral corticospinal tracts and commissural callosal fibres. The current study using an unprecedented number of subjects has revealed more widespread changes. By altering the significance threshold for group differences, a disease-specific pathological pattern of regional involvement was identified which is consistent with post mortem histopathology findings (Braak et

al., 2013). A deeper exploration of the data in relation to phenotype would be a logical next step but requires the provision of more detailed clinical information. The ALSFRS-R score is based upon physical (motor) activities of daily living and is not obviously sensitive to frontal or hippocampal (non-motor) involvement. Nonetheless, mild ALS-FRS-R compared to moderate and severe ALS-FRS-R demonstrated pathological extension from pure CST involvement to involve the wider white matter.

Factors known to directly influence the FA are the voxel size (Oouchi et al., 2007) and participant age (Salat et al., 2005; Lim et al., 2013). Indirect influencing factors on FA (via the signal-to-noise-ratio) are the field strength, the number of gradients, the pulse sequence, and further site specific factors. In DTI, multisite studies appear to be the best solution in order to improve the statistical power in investigation. Recent DTI studies reported replicability, reliability, and stability of DTI-based FA measurements in multisite environments with common acquisition protocols. These studies include a study with 26 patients with Alzheimer's Disease and 12 controls on 16 scanners (Teipel et al., 2011), a study with 9 controls on 2 scanners (Vollmar et al., 2010), and a study with 2 controls on 5 scanners (Fox et al., 2012). Additional studies with harmonized DTI protocols have already been performed in Alzheimer's disease (Jovicich et al., 2014) as well as in Huntington's disease (Müller et al., 2014). A framework for the analysis of phantom data in multicenter DTI studies has been provided previously (Walker et al., 2013). Reproducibility of DTI metrics has been recently tested in a sample of healthy controls at two identical scanners by Veenith et al. (2013) who reported that the within and between session reproducibility was lower than the values for intersubject variability. The initial suggestions on how to correct for differences in FA maps with different protocols were recently published (Dyrba et al., 2013; Rosskopf et al., 2015). Common acquisition protocols but involving different subjects were investigated for groupwise FA differences between patients and controls on systematic between-site differences (Müller et al., 2013a). During the pooling process, a number of well-defined parameters that confound the FA results could be regressed out. Nevertheless, to some extent, residual site-specific FA-influencing factors might be identified. That way, matrices for regressing out FA-influencing factors could be applied in the identical manner to FA-maps of ALS-patients. This methodological framework could easily be adapted to further DTI metrics, e.g. radial-, axial-, or mean-diffusivity.

A limitation of this study compared to other multicentre studies of neurodegenerative diseases (e.g. the PADDINGTON study in Huntington´s Disease (Hobbs et al., 2012) or the Alzheimer's Disease Neuroimaging Initiative (ADNI) (Nir et al., 2013)) is the heterogeneous nature of DTI data resource in terms of magnetic field strength and acquisition sequence parameters used across the sites. It would be advantageous in a future prospective multi-site study to try to harmonise as many data acquisition sequence parameters as possible. A further potential limitation of the current approach is

the limited number of control data sets per centre which may be not homogeneous over sites, and might lead to false or over-correction. However, N=20 (which is the case in seven out of the eight centers) has been a standard control sample size in single-site studies (see e.g. Filippini et al.,2010; Agosta et al., 2010; Müller et al., 2012; Chio et al., 2014). As the ratio patients/controls did not differ strongly between different centers, a systematic center difference would be averaged out in the multi-site group comparison.

By this multi-centre approach involving DTI datasets from more than 250 patients, it was possible to reveal the in vivo pathoanatomy of ALS non-invasively, which was found to be in plausible agreement with post mortem neuroanatomical studies (Smith et al., 1960 ; Braak et al., 2013 ; Brettschneider et al., 2013). This study represents a framework for mapping ALS-specific white matter tract alterations using DTI, and provides encouragement for its extension to other neurodegenerative diseases. In other diseases with emerging evidence of a consistent pathological pattern of spread (Jucker and Walker, 2013), the white matter tract pathology will be closer to the underlying pathology than clusters of regional atrophy, and thus the DTI metrics have the potential to serve as read-outs and biomarkers of disease and its progression for future clinical trials.

Acknowledgements

NISALS contributors:

Abdulla, Susanne, Department of Neurology, Hannover Medical School, Germany

Agosta, Federica, Neuroimaging Research Unit, Scientific Institute San Raffaele, Milan, Italy

Ajroud-Driss, Senda, Neurology, Northwestern University, USA

Atassi, Nazem, Neurology, Massachusetts General Hospital, USA

Bastin, Mark, Brain Imaging Research Centre, Centre for Cognitive Aging and Epidemiology, University of Edinburgh, Edinburgh, United Kingdom

Benatar, Michael, Dept. of Neurology, University of Miami School of Medicine, USA

Brooks, William, Hoglund Brain Imaging Center, University of Kansas Medical Center, USA

Calvo, Andrea, Rita Levi Montalcini Department of Neuroscience, University of Torino, Italy

Cardenas-Blanco, Arturo, Plasticity and Neurodegeneration, DZNE, Germany

Chio, Adriano, University of Turin, Torino, Italy

De Carvalho, Mamede, Instituto de Medicina Molecular, Lisbon, Portugal

Dahnke, Robert, Department of Psychiatry, University Hospital Jena, Jena, Germany

Enzinger, Christian, Department of Neurology, Medical University of Graz, Graz, Austria

Ferraro, Pilar Maria, Neuroimaging Research Unit, Scientific Institute San Raffaele, Milan, Italy

Floeter, Mary Kay, SSPU, EMG section, National Institute of Neurological Disorders and Stroke, US

Foerster, Bradley, Radiology, Division of Neuroradiology, University of Michigan, USA

Gaser, Christian, Department of Psychiatry, Friedrich-Schiller-University of Jena, Jena, Germany

Geraldo, Ana Filipa, Neuroradiology, HSM, Portugal

Gorges, Martin, Department for Neurology, University of Ulm, Ulm, Germany

Grehl, Torsten, Kliniken Bergmannsheil, Bochum, Germany

Groen, Georg, Section Neuropsychology and Functional Imaging, Department of Psychiatry, University of Ulm, Germany

Hardiman, Orla, Department of Neurology, Trinity College Dublin, Dublin, Ireland

Hartung, Viktor, Department of Neurology, University Hospital Jena, Jena, Germany

Jelsone-Swain, Laura, Department of Psychology, University of South Carolina Aiken, USA

Jenkins, Tom, Department of Neurology, Sheffield Institute for Translational Neuroscience, United Kingdom

Kalra, Sanjay, Medicine (Neurology), University of Alberta, Canada

Kasper, Elisabeth, , University of Rostock, Rostock, Germany

Kitzler, Hagen, Dept. of Neuroradiology, Technische Universitaet Dresden, University Hospital, Dresden, Germany

Koritnik, Blaz, Institute of Clinical Neurophysiology, University Medical Centre Ljubljana, Slovenia

Kuzma–Kozakiewicz, Magdalena, Medical University of Warsaw, Poland

LaFleur, Karl, Neurology/Psychiatry, University Medical Center - Utrecht, The Netherlands

Lulé, Dorothée, Neurology, University of Ulm, Ulm, Germany

Machts, Judith, Neurology, German Centre for Neurodegenerative Diseases, DZNE, Rostock, Germany

Meoded, Avner, EMG, NINDS, USA

Pettit, Lewis, Human Cognitive Neuroscience, Psychology–PPLS & Euan MacDonald Centre for MND Research & Centre for Cognitive Aging and Epidemiology, University of Edinburgh, Edinburgh, United Kingdom

Pioro, Erik, Neurology, Cleveland Clinic, USA

Poletti, Barbara, Department of Neurology and Laboratory of Neuroscience, IRCCS Istituto Auxologico Italiano, Italy

Pradat, Pierre-Francois, Department of Neurology, Pitie-Salpetriere Hospital, France

Prell, Tino, Department of Neurology, University Hospital Jena, Jena, Germany

Proudfoot, Malcolm, Clinical Neuroscience, University of Oxford, United Kingdom

Ratti, Elena, Neurology - Neurological Clinical Research Institute (NCRI), Massachusetts General Hospital, USA

Riva, Nilo, Neurology, San Raffaele Scientific Institute, Italy

Robberecht, Wim, Vlaams Instituut voor Biotechnologie, Leuven, Belgium

Ropele, Stefan, Department of Neurology, Medical University of Graz, Graz, Austria

Salachas, Francois, Assistance Publique-Hopitaux de Paris, France

Schmidt, Ruben, Neurology, UMC Utrecht, The Netherlands

Schmidt-Wilcke, Kliniken Bergmannsheil, Bochum, Germany

Schuster, Christina, Trinity College Dublin, Ireland

Shaw, Pamela, Sheffield Institute for Translational Neuroscience, Sheffield, United Kingdom

Sherman, Alex, Neurological Clinical Research Institute, Massachusetts General Hospital, USA

Silani, Vincenzo, Department of Neurology-Stroke Unit and Department of Neurology and Laboratory of Neuroscience, IRCCS Istituto Auxologico Italiano, Dino Ferrari Centre, Department of Pathophysiology and Transplantation, Universita degli Studi di Milano, Milan, Italy

Spinelli, Edoardo Gioele, Neurimaging Research Unit, Institute of Experimental Neurology, San Raffaele Scientific Institute, Italy

Teipel, Stefan, Psychosomatik , University of Rostock and German Centre for Neurodegenerative Diseases (DZNE), Rostock, Germany

Van Damme, Philip, Department of Neurology, KU Leuven, Belgium
Van den Berg, Leonard, University Medical Center Utrecht, The Netherlands
Van den Heuvel, Martin, Rudolf Magnus Institute of Neuroscience, University Medical Centre Utrecht, The Netherlands
Verstraete, Esther, Neurology, University Medical Center Utrecht, The Netherlands
Walhout, Renée, Neurology, University Medical Center Utrecht, The Netherlands
Welsh, Robert, Radiology and Psychiatry, University of Michigan, USA
Weber, Markus, Kantonsspital St.Gallen, Switzerland,
Westeneng, Henk-Jan, Neurology, University Medical Center Utrecht, The Netherlands
Wittstock, Matthias, Department of Neurology, University of Rostock and DZNE, German Centre for Neurodegenerative Disorders, Rostock, Germany
Yunusova, Yana, Speech-Language Pathology, University of Toronto, Canada

The data acquisition at the University of Miami was funded by the National Insititutes of Health (USA) grant R01 NS060874.
The data acquisition at the University of Ulm was supported by the German Research Foundation (Deutsche Forschungsgemeinschaft, DFG Grant Number LU 336/15-1) and the German Network for Motor Neuron Diseases (BMBF 01GM1103A).
The image acquisition in Edinburgh was performed at the Brain Research Imaging Centre, University of Edinburgh, a center in the SINAPSE Collaboration and was funded by the Silvia Aitken CharitableTrust.
The image acquisition in Milan is granted by the Italian Ministry of Health (Grant #RF-2010-2313220).
The project was supported through the following funding organisations under the aegis of JPND - www.jpnd.eu (Project grant SOPHIA): France, Agence Nationale de la Recherche (ANR); Germany, Bundesministerium für Bildung und Forschung (BMBF); Ireland, Health Research Board (HRB); Italy, Ministero della Salute; The Netherlands, The Netherlands Organisation for Health Research and Development (ZonMw); Poland, Narodowe Centrum Badań i Rozwoju; Portugal, Fundação a Ciência e a Tecnologia; Switzerland, Schweizerischer Nationalfonds zur Förderung der wissenschaftlichen Forschung (SNF); United Kingdom, Medical Research Council (MRC).

References

Agosta F, Chiò A, Cosottini M, De Stefano N, Falini A, Mascalchi M, et al. The present and the future of neuroimaging in amyotrophic lateral sclerosis. AJNR Am J Neuroradiol. 2010; 31: 1769-77.

Agosta F, Pagani E, Petrolini M, Caputo D, Perini M, Prelle A, et al. Assessment of white matter tract damage in patients with amyotrophic lateral sclerosis: a diffusion tensor MR imaging tractography study. AJNR Am J Neuroradiol. 2010; 31: 1457-61.

Bede P and Hardiman O. Lessons of ALS imaging: Pitfalls and future directions - A critical review. Neuroimage Clin. 2014; 4: 436-43.

Braak H, Brettschneider J, Ludolph AC, Lee VM, Trojanowski JQ, Del Tredici K. Amyotrophic lateral sclerosis - a model of corticofugal axonal spread. Nat Rev Neurol. 2013; 9: 708-14.

Brettschneider J, Del Tredici K, Toledo JB, et al. Stages of pTDP-43 pathology in amyotrophic lateral sclerosis. Ann Neurol. 2013; 74: 20-38.

Cedarbaum JM, Stambler N, Malta E, Fuller C, Hilt D, Thurmond B, et al. The ALSFRS-R: a revised ALS functional rating scale that incorporates assessments of respiratory function. BDNF ALS Study Group (Phase III). J Neurol Sci. 1999; 169: 13-21.

Chiò A, Pagani M, Agosta F, Calvo A, Cistaro A, Filippi M. Neuroimaging in amyotrophic lateral sclerosis: insights into structural and functional changes. Lancet Neurol. 2014;13:1228-40

Dyrba M, Ewers M, Wegrzyn, Kilimann I, Plant C, Oswald A, et al. Robust automated detection of microstructural white matter degeneration in Alzheimer's disease using machine learning classification of multicenter DTI data. PLoS One. 2013; 8: e64925.

Filippini N, Douaud G, Mackay CE, Knight S, Talbot K, Turner MR. Corpus callosum involvement is a consistent feature of amyotrophic lateral sclerosis. Neurology. 2010; 75: 1645-52.

Foerster BR, Welsh RC, Feldman EL. 25 years of neuroimaging in amyotrophic lateral sclerosis.

Nat Rev Neurol. 2013a; 9: 513-24.

Foerster BR, Dwamena BA, Petrou M, Carlos RC, Callaghan BC, Churchill CL, et al. Diagnostic accuracy of diffusion tensor imaging in amyotrophic lateral sclerosis: a systematic review and individual patient data meta-analysis. Acad Radiol. 2013b; 20: 1099-106.

Fox RJ, Sakaie K, Lee JC, Debbins JP, Liu Y, Arnold DL, et al. A validation study of multicenter diffusion tensor imaging: reliability of fractional anisotropy and diffusivity values. AJNR Am J Neuroradiol. 2012; 33: 695-700.

Genovese CR, Lazar NA, Nichols T. Thresholding of statistical maps in functional neuroimaging using the false discovery rate. Neuroimage 2002; 15: 870-8.

Hobbs NZ, Cole JH, Farmer RE, Rees EM, Crawford HE, Malone IB, et al. Evaluation of multi-modal, multi-site neuroimaging measures in Huntington's disease: Baseline results from the PADDINGTON study. Neuroimage Clin. 2012; 2: 204-11.

Jovicich J, Marizzoni M, Bosch B, Bartrés-Faz D, Arnold J, Benninghoff J, Wiltfang J, et al. Multisite longitudinal reliability of tract-based spatial statistics in diffusion tensor imaging of healthy elderly subjects. Neuroimage. 2014; 101: 390-403.

Jucker M, Walker LC. Self-propagation of pathogenic protein aggregates in neurodegenerative diseases. Nature. 2013; 501: 45-51.

Kassubek J, Ludolph AC, Müller HP. Neuroimaging of motor neuron diseases. Ther Adv Neurol Disord. 2012; 5: 119-27.

Kassubek J, Müller HP, Del Tredici K, Brettschneider J, Pinkhardt EH, Lulé D, et al. Diffusion tensor imaging analysis of sequential spreading of disease in amyotrophic lateral sclerosis confirms patterns of TDP-43 pathology. Brain. 2014; 137: 1733-40.

Keil C, Prell T, Peschel T, Hartung V, Dengler R, Grosskreutz J. Longitudinal diffusion tensor imaging in amyotrophic lateral sclerosis. BMC Neurosci. 2012; 13: 141-52.

Kunimatsu A, Aoki S, Masutani Y, Abe O, Hayashi N, Mori H, et al. The optimal trackability

threshold of fractional anisotropy for diffusion tensor tractography of the corticospinal tract. Magn Reson Med Sci 2004; 3: 11-7.

Le Bihan D, Mangin JF, Poupon C, Clark CA, Pappata S, Molko N, et al. Diffusion tensor imaging: concepts and applications. J Magn Reson Imaging 2001; 13: 534-46.

Lim S, Han CE, Uhlhaas PJ, Kaiser M. Preferential Detachment During Human Brain Development: Age- and Sex-Specific Structural Connectivity in Diffusion Tensor Imaging (DTI) Data. Cereb Cortex. 2013 .

Menke RA, Körner S, Filippini N, Douaud G, Knight S, Talbot K, et al. Widespread grey matter pathology dominates the longitudinal cerebral MRI and clinical landscape of amyotrophic lateral sclerosis. Brain. 2014; 137: 2546-55.

Müller HP, Süssmuth SD, Landwehrmeyer GB, Ludolph A, Tabrizi SJ, Kloppel S, et al. Stability effects on results of diffusion tensor imaging analysis by reduction of the number of gradient directions due to motion artifacts: an application to presymptomatic Huntington's disease. PLoS Curr. 2011 PMID: 22307262

Müller HP, Unrath A, Huppertz HJ, Ludolph AC, Kassubek J. Neuroanatomical patterns of cerebral white matter involvement in different motor neuron diseases as studied by diffusion tensor imaging analysis. Amyotroph Lateral Scler. 2012; 13: 254-64.

Müller HP, Grön G, Sprengelmeyer R, Kassubek J, Ludolph AC, Hobbs N, et al. Evaluating multicentre DTI data in Huntington's disease on site specific effects: An ex post facto approach. Neuroimage Clin. 2013a; 2: 161-7.

Müller HP, Kassubek J. Diffusion tensor magnetic resonance imaging in the analysis of neurodegenerative diseases. J Vis Exp. 2013b; 77.

Müller HP, Kassubek J, Grön G, Sprengelmeyer R, Ludolph AC, Klöppel S, et al. Impact of the control for corrupted diffusion tensor imaging data in comparisons at the group level: an application in Huntington disease. Biomed Eng Online. 2014; 13: 128.

Nir TM, Jahanshad N, Villalon-Reina JE, Toga AW, Jack CR, Weiner MW, et al. Alzheimer's

Disease Neuroimaging Initiative (ADNI). Effectiveness of regional DTI measures in distinguishing Alzheimer's disease, MCI, and normal aging. Neuroimage Clin. 2013; 3: 180-95.

Oouchi H, Yamada K, Sakai K, Kizu O, Kubota T, Ito H, et al. Diffusion anisotropy measurement of brain white matter is affected by voxel size: underestimation occurs in areas with crossing fibers. AJNR Am J Neuroradiol. 2007; 28: 1102-6.

Pettit LD, Bastin ME, Smith C, Bak TH, Gillingwater TH, Abrahams S. Executive deficits, not processing speed relates to abnormalities in distinct prefrontal tracts in amyotrophic lateral sclerosis. Brain. 2013; 136: 3290-304.

Rosskopf J, Müller HP, Dreyhaupt J, Gorges M, Ludolph AC, Kassubek J. Ex post facto assessment of diffusion tensor imaging metrics from different MRI protocols: preparing for multicentre studies in ALS. Amyotroph Lateral Scler Frontotemporal Degener. 2015, 9: 1-10.

Salat DH, Tuch DS, Greve DN, van der Kouwe AJ, Hevelone ND, Zaleta AK, et al. Age-related alterations in white matter microstructure measured by diffusion tensor imaging. Neurobiol Aging. 2005; 26: 1215-27.

Sarro L, Agosta F, Canu E, Riva N, Prelle A, Copetti M, et al. Cognitive functions and white matter tract damage in amyotrophic lateral sclerosis: a diffusion tensor tractography study. AJNR Am J Neuroradiol. 2011; 32: 1866-72.

Smith MC. Nerve fibre degeneration in the brain in amyotrophic lateral sclerosis. J Neurol Neurosurg Psychiatry. 1960; 23: 269–82.

Teipel SJ, Reuter S, Stieltjes B, Acosta-Cabronero J, Ernemann U, Fellgiebel A, et al. Multicentre stability of diffusion tensor imaging measures: a European clinical and physical phantom study. Psychiatry Res. 2011; 194: 363-71.

Turner MR, Kiernan MC, Leigh PN, Talbot K. Biomarkers in amyotrophic lateral sclerosis. Lancet Neurol. 2009; 8: 94-109.

Turner MR, Grosskreutz J, Kassubek J, Abrahams S, Agosta F, Benatar M, et al. Towards a

neuroimaging biomarker for amyotrophic lateral sclerosis. Lancet Neurol. 2011; 10: 400-3.

Turner MR, Agosta F, Bede P, Govind V, Lulé D, Verstraete E. Neuroimaging in amyotrophic lateral sclerosis. Biomark Med. 2012; 6: 319-37.

Turner MR, Benatar M. Ensuring continued progress in biomarkers for amyotrophic lateral sclerosis. Muscle Nerve. 2015; 51: 14-8.

Veenith TV, Carter E, Grossac J, Newcombe VF, Outtrim JG, Lupson V, et al. Inter subject variability and reproducibility of diffusion tensor imaging within and between different imaging sessions. PLoS One. 2013; 8: e65941.

Vollmar C, O'Muircheartaigh J, Barker GJ, Symms MR, Thompson P, Kumari V, et al. Identical, but not the same: intra-site and inter-site reproducibility of fractional anisotropy measures on two 3.0T scanners. Neuroimage. 2010; 51: 1384-94.

Walker L, Curry M, Nayak A, Lange N, Pierpaoli C. Brain Development Cooperative Group. A framework for the analysis of phantom data in multicenter diffusion tensor imaging studies. Hum Brain Mapp. 2013; 34: 2439-54.

Figures and Table

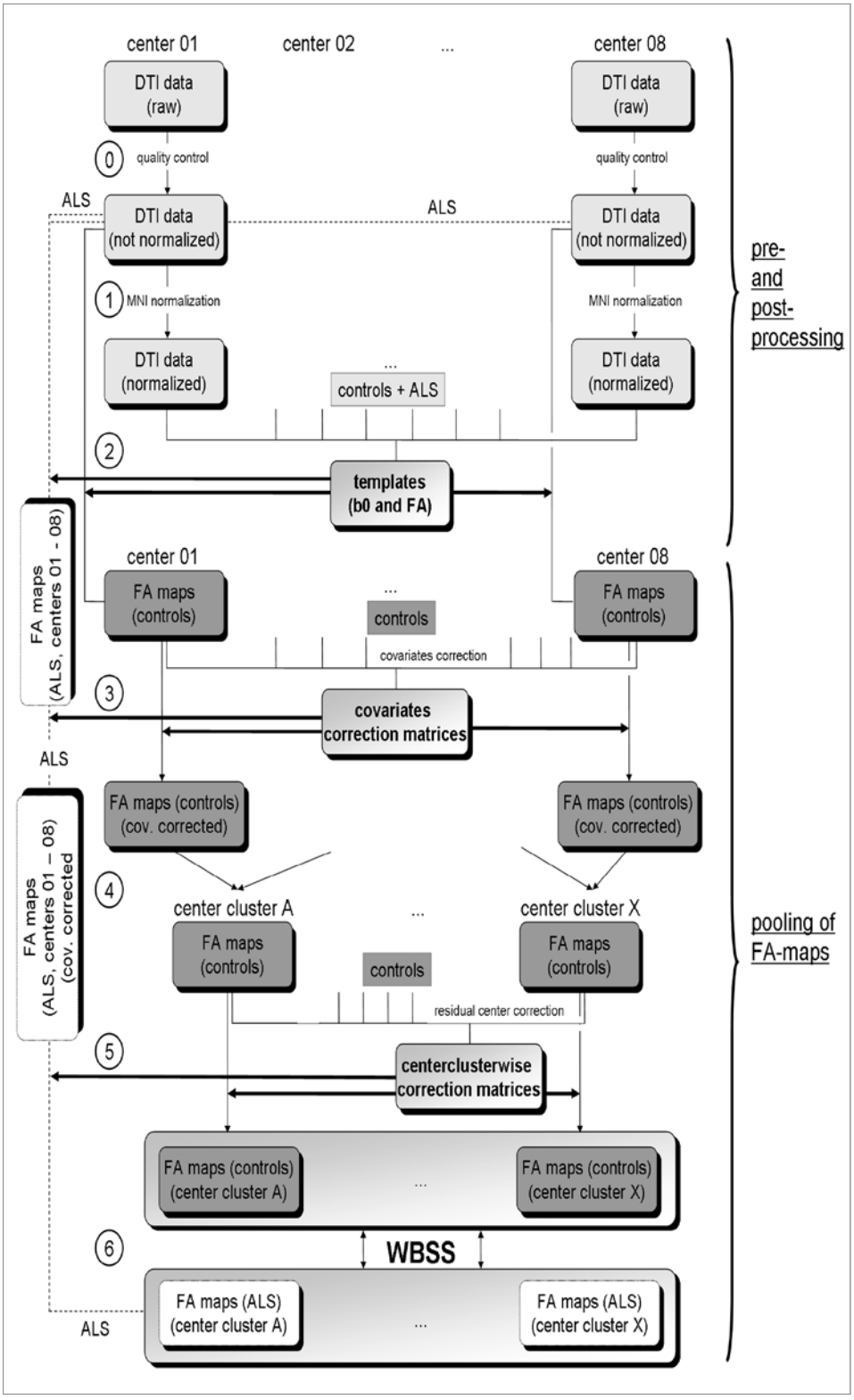

Figure 1: Schematic pre-and postprocessing and pooling of data. Upper panel (pre- and postprocessing): Data from each site underwent a quality assessment (0) where corrupted gradient directions in single DTI data sets (ALS and controls) were excluded for further analysis. In the next step (1), by a standardized iterative stereotaxic normalization process (using study specific DTI template sets), FA maps (ALS and controls) were transformed into stereotaxic standard space (MNI

space). For the comparison of centres, a study-specific template set (b0 and FA) was created with equal weighting of centres, ALS patients, and controls; then stereotaxic normalization was performed repeatedly with these equally weighted templates (2). Lower panel (pooling of FA maps): For controls' FA maps, the covariates voxel size, age, number of GD, B0, and TE were regressed out and a corrected FA-map set consisting of FA maps of all controls was derived (3). The identical 3D-matrices for regressing out covariates in the control data sets were then applied to FA maps of ALS-patients (3). In the following step, centrewise pooling of FA maps of controls was performed by creating groups of centres that showed no relevant differences in FA maps of controls (4); centre grouping was performed simultaneously also for FA-maps of ALS-patients. Residual accompanying centre-specific influences e.g. timing of scan, phenotype variations within the diagnosis of ALS, were defined as inter-centre effects and, in a final step, 3D linear correction matrices were calculated for the centres (5). The identical correction matrices were then applied to FA maps of ALS-patients. Finally, whole brain-based spatial statistics (WBSS) (6) was applied to the pooled FA maps of ALS patients and controls. Results were corrected for multiple comparisons at $p < 0.05$.

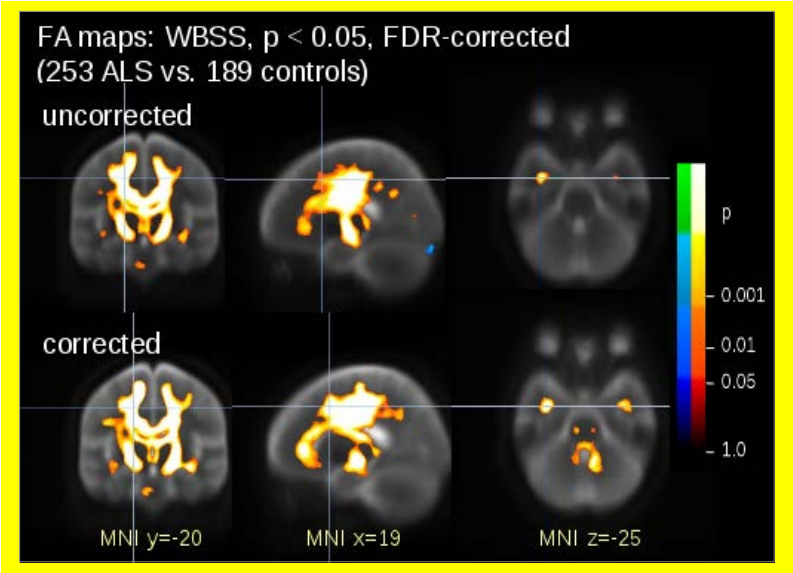

Figure 2: Cross-sectional comparison of FA maps of ALS patients vs. controls. Whole brain-based spatial statistics (WBSS) of uncorrected (upper panel) and corrected (lower panel) FA maps of 253 ALS-patients vs. 189 controls, $p < 0.05$, corrected for multiple comparisons. Clusters of regional decrease were displayed on an averaged b0-template as background.

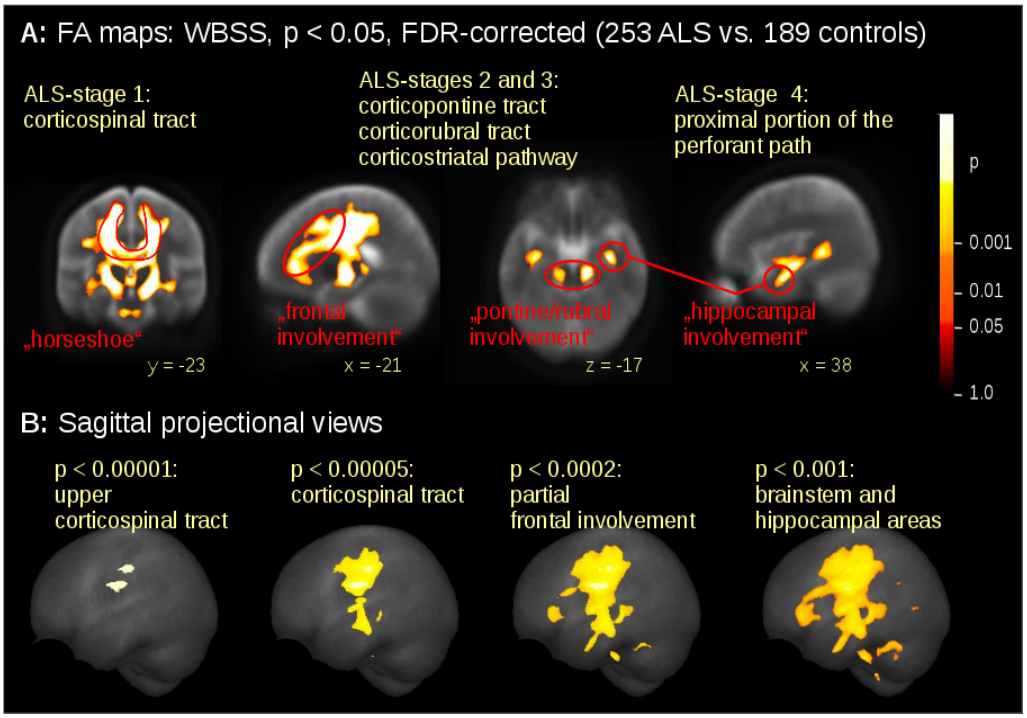

Figure 3: Cross-sectional comparison of FA maps of ALS patients vs. controls. Whole brain-based spatial statistics (WBSS) of FA maps of 253 ALS-patients vs. 189 controls, $p < 0.05$, corrected for multiple comparisons. Clusters of regional decrease were displayed on an averaged b0-template as background. **(A)** Selective slice representations of the ALS-characteristic "horseshoe" (ALS-stage 1, corticospinal tract and corpus callosum), alterations of frontal lobes and of rubral and pontine areas (ALS-stages 2 and 3, corticopontine tract, corticorubral tract, and corticostriatal pathway), and alterations of hippocampal regions (ALS-stage 4, proximal portion of the perforant path). **(B)** Projectional sagittal views for different display thresholds. Highest significance ($p < 0.00001$) was found in the upper corticospinal tracts, followed by (also high) significance ($p < 0.00005$) in both corticospinal tracts. Display of lower significance thresholds shows involvement of alterations of the frontal lobes ($p < 0.0002$) and lowest significance threshold ($p < 0.001$) shows broader affectations to the frontal lobes and also to hippocampal regions.

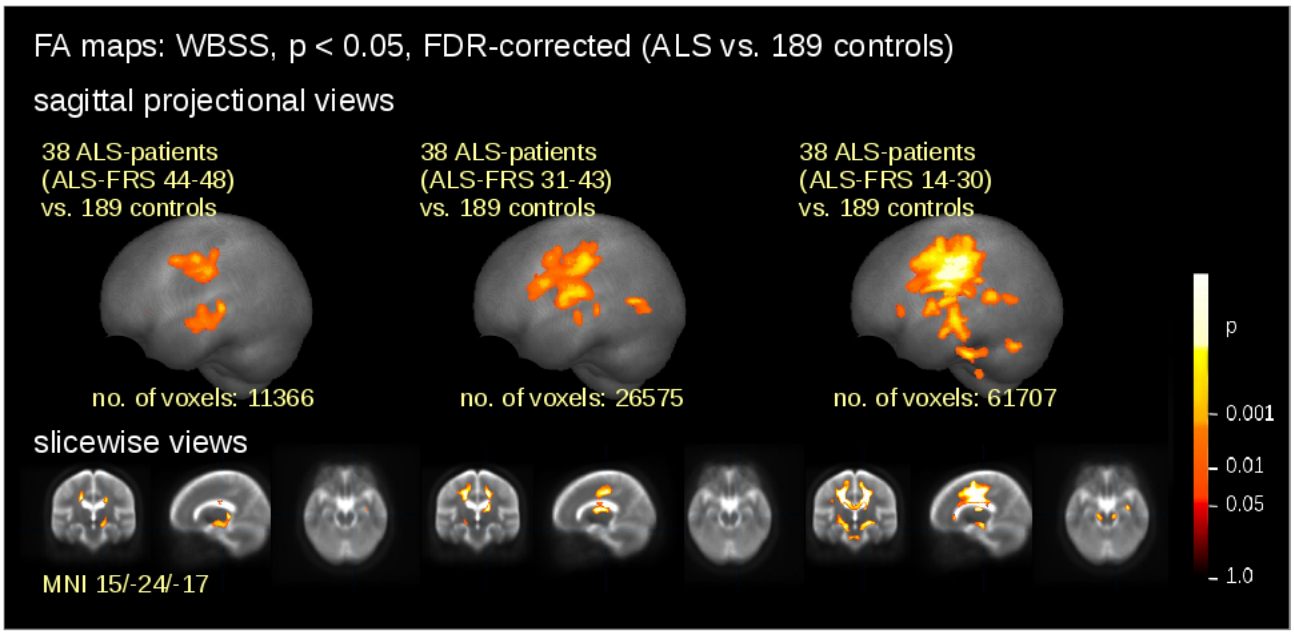

Figure 4: Comparison of FA maps of ALS patients vs. controls as stratified for disease severity (ALS-FRS-R). Whole brain-based spatial statistics (WBSS) of FA maps of ALS-patient subgroups as stratified for ALS-FRS-R values vs. controls at $p < 0.05$, corrected for multiple comparisons. Clusters of regional decreases are displayed on an averaged b0-template. Projectional sagittal views: ALS-FRS-R range 44-48 (38 ALS patients vs. 189 controls), ALS-FRS-R range 31-43 (38 ALS patients vs. 189 controls), and ALS-FRS-R range 14-30 (38 ALS patients vs. 189 controls).

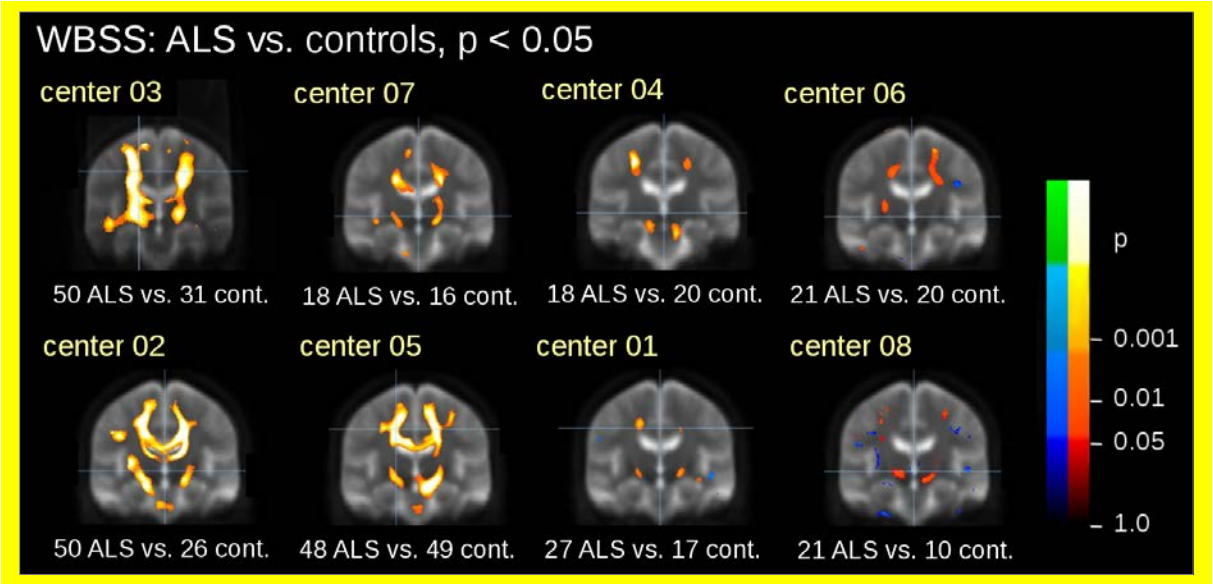

Supplementary Figure 1: Whole-brain-based voxelwise analysis (WBSS) of single centres' FA maps. Comparison of ALS patients vs. controls of single centres' FA maps (without correction of confounding multicentric factors) showed FA decreases mainly localized along the CST, $p < 0.05$, FDR-corrected. Clusters of regional decrease are displayed on an averaged b0-template as background (coronal slice at MNI y=-20). Results for centers 06 and 08 were uncorrected (after correction for multiple comparisons at $p < 0.05$, for these two centers no clusters were found).

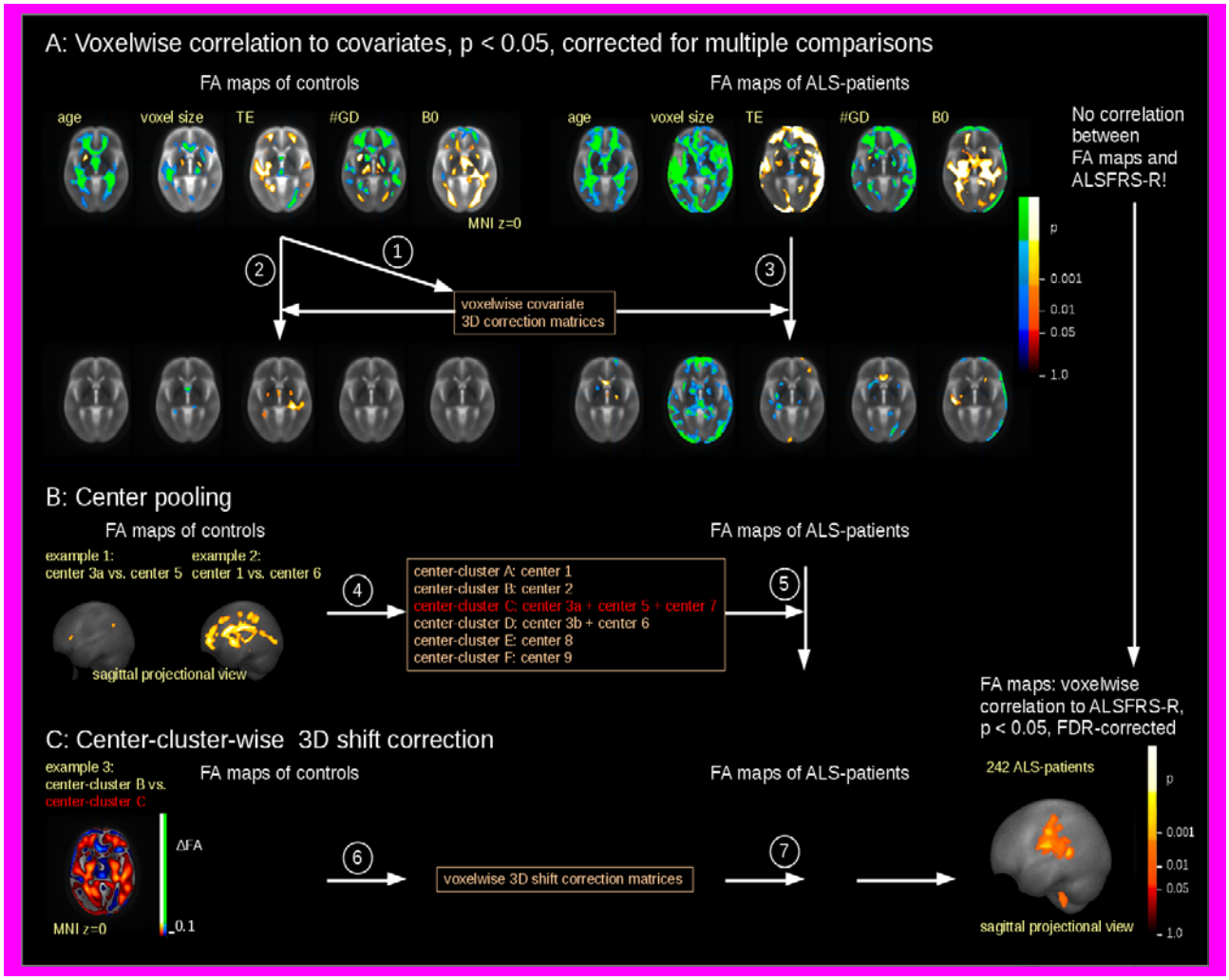

Supplementary Figure 2: Voxelwise correction of confounding factors. (A) FA maps of controls showed significant correlations ($p < 0.05$, corrected for multiple comparisons) to the covariates voxel size, age, number of GD, B0, and TE (upper panel, left). After regressing out these covariates by setting up covariate 3D correction matrices (1) only small clusters of significance remained (lower panel, left) (2). The application of the correction matrices to FA maps of ALS patients (upper panel, right) also reduced the dependency on the covariates voxel size, age, number of GD, B0, and TE (lower panel, right) (3). (B) Pooling of centers. Centres were merged into centre-clusters if the number of significant voxels in group comparison of controls is below a threshold of 10 000 voxels – see examples 1 and 2: center 3a and center 5 could be pooled, whereas center 1 and center 6 could not be pooled.. Centres FA maps were merged into centre-clusters for FA maps of controls (4) and for FA maps of ALS patients (5). (C) Finally, residual accompanying site-specific influences were corrected by 3D linear correction matrices for FA maps of controls (6) and for FA maps of ALS

patients (7). Right: Voxelwise correlation of ALS-FRS-R to FA values (242 ALS patients), $p < 0.05$, corrected for multiple comparisons.

centre	ALS (m/f)	mean age / years	controls (m/f)	mean age / years	TR / s	TE / ms	vsize (x/y/z) / mm	vsize / mm^3	no. GD	B0 / T
01	27 (18/9)	61	17 (8/9)	58	7.8	97	1.3/1.3/2.5	3.9	33	1.5
02	50 (29/21)	60	26 (11/15)	49	10.0	94	2.0/2.0/2.0	8.0	31	3.0
03a*	28 (17/11)	57	14 (8/6)	57	8.0	93	1.5/1.5/2.2	5.0	13	1.5
03b*	22 (8/14)	64	17 (9/8)	62	8.0	95	2.0/2.0/2.8	11.2	52	1.5
04	18 (10/8)	65	20 (9/11)	64	5.1	85	2.0/2.0/2.0	8.2	92	3.0
05	48 (27/21)	61	49 (27/22)	59	7.6	59	2.2/2.2/2.5	12.0	34	3.0
06	21 (14/7)	54	20 (9/10)	51	11.8	80	1.1/1.1/2.2	2.7	52	3.0
07	18 (6/12)	61	16 (9/7)	60	9.0	80	0.9/0.9/2.5	2.2	33	3.0
08	21 (11/10)	59	10 (6/4)	66	16.5	98	2.0/2.0/2.0	8.0	71	1.5
total or mean	**253 (140/113)**	**60**	**189 (96/93)**	**58**	n.a.	n.a.	n.a.	n.a.	n.a	n.a.

Table 1: Number and demographics of subjects and DTI scanning protocols of the multi-centre setting. Age and voxelsize influence directly FA. Indirect influence on FA maps (via signal-to-noise ratio of recorded DTI data sets) results from the number of gradient directions (GD), the field strength (B0) and echo time (TE). *Data using two different protocols from the same centre were treated separately.